

Constraints on Very High Energy gamma-ray emission from Gamma-Ray Bursts

R. Atkins,^{1,2} W. Benbow,^{3,4} D. Berley,⁵ E. Blaufuss,⁵ D. G. Coyne,³ T. DeYoung,^{3,5}
B. L. Dingus,⁶ D. E. Dorfan,³ R. W. Ellsworth,⁷ L. Fleysher,⁸ R. Fleysher,⁸
M. M. Gonzalez,¹ J. A. Goodman,⁵ E. Hays,^{5,9,10} C. M. Hoffman,⁶ L. A. Kelley,³
C. P. Lansdell,⁵ J. T. Linnemann,¹¹ J. E. McEnery,^{1,12} A. I. Mincer,⁸ M. F. Morales,^{3,13}
P. Nemethy,⁸ D. Noyes,⁵ J. M. Ryan,¹⁴ F. W. Samuelson,¹⁵ P. M. Saz Parkinson,³
A. Shoup,¹⁶ G. Sinnis,⁶ A. J. Smith,⁵ G. W. Sullivan,⁵ D. A. Williams,³ M. E. Wilson,¹
X. W. Xu⁶ and G. B. Yodh¹⁶

Received _____; accepted _____

¹ Department of Physics, University of Wisconsin, 1150 University Ave, Madison, WI 53706

² Current address: Department of Physics, University of Utah, 115 South 1400 East, Salt Lake City, UT 84112

³ Santa Cruz Institute for Particle Physics, University of California, 1156 High Street, Santa Cruz, CA 95064

⁴ Current address: Max-Planck-Institut für Kernphysik, Postfach 103980, D-69029 Heidelberg, Germany

⁵ Department of Physics, University of Maryland, College Park, MD 20742

⁶ Group P-23, Los Alamos National Laboratory, P.O. Box 1663, Los Alamos, NM 87545

⁷ Department of Physics and Astronomy, George Mason University, 4400 University Drive, Fairfax, VA 22030

⁸ Department of Physics, New York University, 4 Washington Place, New York, NY 10003

⁹ Current address: High Energy Physics Division, Argonne National Laboratory, Argonne, IL 60439

¹⁰ Current address: Enrico Fermi Institute, University of Chicago, Chicago, IL, 60637

¹¹ Department of Physics and Astronomy, Michigan State University, 3245 BioMedical Physical Sciences Building, East Lansing, MI 48824

¹² Current address: NASA Goddard Space Flight Center, Greenbelt, MD 20771

¹³ Current address: Massachusetts Institute of Technology, Building 37-664H, 77 Massachusetts Avenue, Cambridge, MA 02139

¹⁴ Department of Physics, University of New Hampshire, Morse Hall, Durham, NH 03824

¹⁵ Office of Science and Engineering Laboratories, Center for Devices and Radiological Health, U.S. Food and Drug Administration.

¹⁶ Department of Physics and Astronomy, University of California, Irvine, CA 92697

Version of 11 March 2005

ABSTRACT

The Milagro gamma-ray observatory employs a water Cherenkov detector to observe extensive air showers produced by high energy particles interacting in the Earth's atmosphere. Milagro has a wide field of view and high duty cycle, monitoring the northern sky almost continuously in the 100 GeV to 100 TeV energy range. Milagro is, thus, uniquely capable of searching for very high-energy emission from gamma-ray bursts (GRBs) during the prompt emission phase. Detection of >100 GeV counterparts would place powerful constraints on GRB mechanisms. Twenty-five satellite-triggered GRBs occurred within the field of view of Milagro between January 2000 and December 2001. We have searched for counterparts to these GRBs and found no significant emission from any of the burst positions. Due to the absorption of high-energy gamma rays by the extragalactic background light, detections are only expected to be possible for redshifts less than ~ 0.5 . Three of the GRBs studied have measured redshifts. GRB 010921 has a redshift low enough (0.45) to allow an upper limit on the fluence to place an observational constraint on potential GRB models.

Subject headings: gamma rays: bursts — gamma rays: observations

1. Introduction

The search for prompt very high energy (VHE) emission (>100 GeV) from gamma-ray bursts (GRBs) is motivated by both experimental observations and theoretical predictions, and its detection could allow us to constrain GRB emission models. Although no observation has yet conclusively demonstrated VHE emission from any single burst, there have been several indications of emission at these high energies.

Milagrito, a prototype of Milagro, reported evidence for emission above 650 GeV from GRB 970417a, with a (post-trials) probability of 1.5×10^{-3} of being a background fluctuation (Atkins et al. 2000a, 2003a). This search included 53 other bursts from which no significant emission was detected. The Tibet air shower array reported a correlation between ~ 10 TeV air showers and a sample of 57 GRBs detected by the Burst And Transient Source Experiment (BATSE) (Amenomori et al. 1996), although no significant signal was detected from any of the directions of the individual BATSE bursts. Evidence at about the 3 sigma level with HEGRA has been published for emission above 20 TeV from GRB 920925c (Padilla et al. 1998). Follow-up observations above 250 GeV by the Whipple atmospheric Cherenkov telescope (Connaughton et al. 1997) did not find any high energy afterglow for 9 bursts studied. Because this search involved slewing the Whipple telescope into position after receiving a burst alert from BATSE (for these 9 bursts the delays ranged from 2 minutes to 56 minutes), only delayed emission could be detected. In addition, the small field of view of Whipple (3°), compounded with the relatively large uncertainty in the BATSE location of the bursts ($\sim 10^\circ$ in diameter) meant the process of searching the burst region required multiple pointings, taking a 3 hour observing cycle and still covering less than 50% of the actual BATSE error box, further hampering any early detection of TeV emission (Connaughton et al. 1997).

Although most GRBs have been detected in the energy range between 20 keV and 1 MeV, a few bursts have been observed at energies above 100 MeV by EGRET, including the detection of an 18 GeV photon from GRB 940217, over 90 minutes after the start of the burst (Hurley et al. 1994), indicating both that the spectra of some GRBs extend to at least GeV energies and that this emission may be delayed (Dingus 1995, 2001).

Recently, a second spectral component was found in GRB 941017 (Gonzalez et al. 2003). This second component extended up to at least 200 MeV, and its flux decayed more

slowly than the lower energy component. It is still unknown to how high in energy the second component extends. It is not clear whether it is similar to the high energy peak seen in TeV sources and attributed to inverse Compton emission or the result of a completely different mechanism. The second component has a very hard, power law spectrum, with a differential photon index of -1 ± 0.3 , which if extrapolated to 100 GeV would make the burst extremely bright, with a fluence greater than $10^{-3} \text{ erg s}^{-1} \text{ cm}^{-2}$.

The observation of VHE emission from GRBs is hindered by collisions between the gamma rays and the extragalactic infrared background light (EBL), producing electron-positron pairs (Nikishov 1961). The degree of gamma-ray extinction from this effect is uncertain, because the amount of EBL is not well known. Direct measurements of the extragalactic background light have proven difficult, because of the foreground contribution from the Galaxy. There are several models of the extinction (Primack et al. 1999; Stecker & de Jager 1998; De Jager & Stecker 2002), which are similar in their general features because of the constraints from the available data. Recent progress in the field has come about due to the accurate determination of the cosmological parameters, as well as a greatly increased knowledge of the luminosity function of galaxies. The most recent model now predicts a somewhat smaller absorption than was previously expected (Primack et al. 2004), with an optical depth predicted to be roughly unity to 500 GeV (10 TeV) gamma rays from a redshift of 0.2 (0.05).

While VHE emission from GRBs has been elusive, it is a natural byproduct of most GRB production models and is often predicted to have a fluence comparable to that at MeV energies (Dermer, Chiang & Mitman 2000; Pilla & Loeb 1998; Zhang & Mészáros 2001). This is a result of the fact that the MeV emission from GRBs is likely synchrotron radiation produced by energetic electrons within the strong magnetic field of a jet with bulk Lorentz factors exceeding 100. In such an environment, the inverse Compton mechanism for

transferring energy from electrons to gamma rays is likely to produce a second higher energy component of GRB emission with fluence possibly peaked at 1 TeV or above. The relative strengths of the synchrotron and inverse Compton emission depend on the environments of the particle acceleration and the gamma ray production.

In this paper, we use the Milagro gamma-ray observatory to search for VHE emission during the prompt emission of GRBs during 2000 and 2001. The GRBs have been detected by one or more of several satellite instruments: BATSE, Rossi X-ray Transient Explorer (RXTE), BeppoSax, High Energy Transient Explorer (HETE), and the Third Interplanetary Network (IPN), and occurred overhead within the field of view of Milagro. The combination of large field of view and high duty cycle make Milagro the best instrument available for conducting this type of search.

2. The Milagro Observatory

Milagro is a TeV gamma-ray detector which uses the water Cherenkov technique to detect extensive air showers produced by very high-energy gamma rays as they traverse the Earth's atmosphere (Atkins et al. 2000b). Milagro is located in the Jemez Mountains of northern New Mexico (35.9° N, 106.7° W) at an altitude of 2630 m above sea level, and has a field of view of ~ 2 sr and a duty cycle of over 90%, making it an ideal all-sky monitor of transient phenomena at very high energies, such as GRBs. The effective area and energy threshold of Milagro are a function of zenith angle, due to the increased atmospheric overburden at larger zenith angles, which tends to attenuate the particles in the air shower before they reach the ground. During the period covered by these observations, the Milagro trigger required that approximately 55 tubes be hit within a 200 ns time window. For more details on Milagro see Atkins et al. (2003b). Figure 1 shows the effective area to gamma rays of Milagro during the years 2000 and 2001. The plot shows the effective area for four

different ranges of zenith angles: $0^\circ\text{--}15^\circ$, $15^\circ\text{--}30^\circ$, $30^\circ\text{--}40^\circ$, and $40^\circ\text{--}45^\circ$, illustrating the drop suffered in effective area at energies below a few TeV for large zenith angles. As can be seen, the sensitivity of Milagro varies slowly with angle out to around 30 degrees and then drops off. The effective area of Milagro ranges from $\sim 10\text{ m}^2$ at 100 GeV to $\sim 10^5\text{ m}^2$ at 10 TeV. Systematic effects result in an uncertainty in the effective area estimated to be no more than 15%. The angular resolution is approximately 0.7 degrees.

The energy response of Milagro is rather broad with no clear point to define as an instrument threshold. To obtain a rough guide of the range of energies to which Milagro is sensitive, we consider a power law spectrum with a differential photon index, α , of -2.4. The energy (E_5) above which 95% of the triggered events from such a spectrum are obtained is approximately 250 GeV, the energy (E_{95}) below which 95% of the triggered events come is 25 TeV, and the median energy is 2.5 TeV. This illustrates both the breadth of the energy response of Milagro, showing that the Milagro Detector is sensitive to a low energy (< 500 GeV) signal.

3. The GRB sample

Table 1 shows a summary of the sample of satellite-triggered GRBs within the field of view (up to zenith angles of 45°) of Milagro during 2000 and 2001. There were three bursts during this two year period which were within the Milagro field of view but occurred when Milagro was not operating. The GRB sample presented here represents approximately a third of all well-localized bursts during that period (Greiner 2004). Of the sample, three have known redshift, with GRB 010921 ($z=0.45$) being the closest. The detector configuration was upgraded starting in 2002 and later bursts will be the topic of a future paper.

The first column in Table 1 is the GRB name, which, following the usual convention, represents the UTC date (YYMMDD) on which the burst took place. The second column gives the instrument(s) that detected the burst. In the case of BATSE, we list the trigger ID. The third column gives the time at which the burst triggered the particular instrument, in Truncated Julian Date (TJD)¹⁷ followed by the UTC second of the day. Column four gives the coordinates (right ascension and declination, in degrees) of the burst. The fifth column gives the uncertainty in the measured location of the burst in degrees. A dashed line implies that the error was small compared to the Milagro point-spread function (PSF). For BATSE bursts, the error radius is the 90% systematic plus statistical uncertainty (added in quadrature). The duration listed in the sixth column is the T90 interval for that burst as reported by the respective instrument teams. When times were reported for several energy bands, we picked the duration in the highest energy band. The seventh column gives the redshift of the GRB, when known. Column eight describes what (if any) afterglows were detected in different energy bands: (O)ptical, (R)adio, or (X)-ray. If an afterglow was observed, it is marked with a check mark, if it was not detected it is marked with a cross, and if no observation was attempted it is marked with a dot. Column nine lists the zenith angle of the burst at Milagro, in degrees. We include only bursts for which the zenith angle was less than 45°. As is implied by Figure 1, the effective area of Milagro at zenith angles greater than 45° becomes negligible in the energy range where we expect GRB emission to be detectable (e.g. < 1 TeV). The remaining columns of the table list the Milagro results and are described later. First, we describe in a little more detail the most interesting GRB from the sample.

¹⁷TJD \equiv Truncated Julian Date = JD - 2,440,000.5 = MJD - 40,000

3.1. GRB 010921

GRB 010921 was detected by the HETE satellite (Ricker et al. 2002), and together with data from the Interplanetary Network (IPN) it was localized to a 310-square-arcmin 3-sigma error box. It had a duration (T_{90}) of 24.6 seconds in the 7–400 keV energy range and a fluence in the 30–400 keV range of 1.02×10^{-5} erg cm^{-2} (Barraud et al. 2003). A variable optical source exhibiting a power law decay measured by the Large Format Camera on the Palomar 200-inch telescope was identified as the afterglow of GRB 010921 (Price et al. 2001). This was superimposed on a bright galaxy, assumed to be the host galaxy, determined to be at $z=0.45$ (Djorgovski et al. 2001). This was the first afterglow detected from a HETE-localized burst. Observations with the Hubble Space Telescope failed to detect a coincident SN to a limit 1.33 magnitude fainter than SN 1998bw at the 99.7% confidence level, making this one of the most sensitive searches for an underlying SN (Price et al. 2003). A radio afterglow was detected by the VLA (Price et al. 2001). This is the first burst in the field of view of Milagro known to be close enough to be potentially detectable above 100 GeV.

The photon spectrum of GRB 010921 in the (7–200) keV range can be fit with a cut-off power law, defined by $dN/dE = AE^\alpha \exp(-E/E_0)$ with α equal to $-1.49_{-0.6}^{+0.7}$, and E_0 equal to 206_{-48}^{+81} keV (Barraud et al. 2003). Sakamoto et al. (2004) obtained slightly different parameters ($\alpha = -1.55_{-0.07}^{+0.08}$, $E_0 = 197_{-31}^{+48}$ keV) by doing a joint spectral fit using WXM in addition to FREGATE data. The data can also be fit by the Band function (Band et al. 1993), defined by $dN/dE = AE^\alpha \exp(-E/E_0)$ for $E \leq (\alpha - \beta)E_0$, and $dN/dE = BE^\beta$ for $E \geq (\alpha - \beta)E_0$, where $B = A[(\alpha - \beta) \times E_0]^{(\alpha - \beta)} \times \exp(\beta - \alpha)$. The best fit parameters obtained from this fit were a low-energy power law index α equal to $-1.52_{-0.09}^{+0.16}$, a high-energy power law index β equal to $-2.33_{-7.67}^{+0.34}$, and E_0 equal to 165_{-59}^{+61} keV (T. Q. Donaghy 2005, private communication). The break energy E_0 is related to the

peak energy in the νF_ν spectrum by the equation $E_p = E_0 \times (2 + \alpha)$. The high-energy power law index, β , is not very well constrained by the HETE data, as seen by the results of the fit. Figure 4 shows the shape of the Band function with β values equal to -1.99, -2.33, and -2.67. As β becomes increasingly negative, the high-energy power law eventually becomes irrelevant in the HETE energy range as the fitting function reduces to the simple absorbed power law.

4. Data Analysis

A search for an excess of events above those expected from the background was made for each of the 25 bursts in the sample. The search was performed for two different durations, T90 (the time interval over which ninety per cent of the flux is observed) and five minutes. Although the value of T90 is derived from observations made at much lower energies than Milagro detects, EGRET showed that this duration is relevant at higher energies too. Four GRBs which were observed with EGRET were among the five brightest bursts observed by BATSE and the significance of the EGRET detections in the T90 interval ranged from 6 to 12 sigma, leading to the speculation that all GRBs might have high energy emission during their respective T90 time intervals, and EGRET simply did not have the sensitivity to detect the rest of the bursts (Dingus 2001). Figure 2 shows the distribution of significances of the 17 well-localized bursts for each T90 duration. The distribution plotted can be fit with a gaussian of mean -0.3 and standard deviation of 1.1. We also chose to search for emission from these GRBs for a duration of five minutes. This timescale was motivated by the recent discovery of a second higher energy component in GRB 941017. While the T90 for that burst was 77 s, the second component (which has a fluence more than three times greater than the fluence in the BATSE energy range alone) has a duration of approximately 211 seconds (Gonzalez et al. 2003).

The total number of events falling within a circular bin of radius 1.6° at the location of the burst was summed for the duration of the burst and is shown in column ten (N_{ON}) of Table 1. An estimate of the number of background events was made by characterizing the angular distribution of the background using two hours of data surrounding the burst (Atkins et al. 2003b). This number is given as N_{OFF} in column eleven of Table 1. The significance of the excess (or deficit) for each burst was evaluated using equation [17] of Li & Ma (1983) and is given in column twelve. For bursts with an uncertainty in the position greater than 0.5° , the search region (given by column five of Table 1) was tiled with an array of overlapping 1.6° radius bins spaced 0.1° apart in right ascension and declination and the numbers given in columns ten and eleven are chosen as the ones giving the excess with maximum significance. Since we do not take into account the total number of bins searched, this number does not represent the significance of detection of this burst and we therefore do not include these values with those of the well-localized bursts, in column 12. No significant excess was found from any burst in the sample. The 99% confidence upper limits on the number of signal events detected, N_{UL} , given the observed N_{ON} and the predicted background N_{OFF} , following the method described by Helene (1983) are given in column thirteen. Finally, we convert the upper limit on the counts into an upper limit on the fluence. Using the effective area of Milagro, A_{eff} , and assuming a differential power-law photon spectrum we integrate in the appropriate energy range and solve for the normalization constant. We chose a spectrum of the form $dN/dE = KE^{-2.4}$ photons/TeV/m². The power law index of 2.4 was chosen as a conservative value for the spectrum. The average spectrum of the four previously mentioned bright bursts observed by EGRET had a differential photon spectrum with index 1.95 ± 0.25 (Dingus 2001) and the average spectrum of high energy blazars can be fit with a simple power law with an index of 2.2 (Weekes, T. C. 2003). The normalization factor K can be calculated by solving the following equation: $N_{\text{UL}} = \int A_{\text{eff}}(dN/dE)dE$. Finally, we integrate the photon

spectrum multiplied by the energy to obtain the corresponding value for the total fluence: $F = \int E(dN/dE)dE$, integrating from 0.25 to 25 TeV.

5. Results

Table 1 shows a summary of GRBs between January 2000 and December 2001 analyzed with Milagro. None of these bursts showed any significant emission in the Milagro data. The 99% confidence upper limits on the fluence for both durations are listed in columns fourteen and fifteen of Table 1 respectively. Note that none of the results listed in the table take into account the effect of absorption from the EBL. For GRB 000301C and GRB 000926, both of which are at $z \sim 2$, we expect essentially all of the TeV emission (if it exists) to be absorbed by the EBL, making the actual upper limit on the emission of TeV gamma rays from these bursts considerably weaker than what is reflected in the table. For all the other bursts (except GRB 010921) there are no redshift measurements, so it is not possible to take this effect into account. The analysis of GRB 010921, which we have described in detail, yields an interesting upper limit, as we describe in the next section.

5.1. GRB 010921

GRB 010921, with a measured redshift of $z=0.45$, is close enough that a potential TeV signal is not totally absorbed by the extragalactic background. Figure 3 shows the effect of various absorption models at a redshift of 0.45 on an $E^{-2.4}$ spectrum which might be expected from a GRB. For an unbroken power law, the energy range from 0.25 TeV to 25 TeV is the sensitive region for Milagro. For a cutoff spectrum, the small amount of sensitivity between 50 and 250 GeV is not negligible, so we now include it. Integrating the product of a normalization constant K times an $E^{-2.4}$ energy spectrum multiplied by the

EBL absorption and effective area in the energy range 0.05–100 TeV and setting it equal to the 99% confidence upper limit on the counts (20.2), allows us to solve for K (2.0×10^{-2} photons $\text{TeV}^{-1} \text{ m}^{-2}$). We then use this normalization constant to compute the unabsorbed fluence. The upper limits obtained are $< 2.9 \times 10^{-5} \text{ erg cm}^{-2}$ for the Primack et al. (2004) model, $5.8 \times 10^{-5} \text{ erg cm}^{-2}$ for the Primack et al. (1999) model, and $< 5.8 \times 10^{-5} \text{ erg cm}^{-2}$ for the “fast evolution” model of Stecker & de Jager (1998) (the more absorptive of their two models). Figure 4 shows the spectrum of GRB 010921 obtained by HETE (in the energy range of 7 to 200 keV, where the data were fitted) as well as the Milagro upper limits. The quantity plotted is $E^2 dN/dE$, and has been evaluated at the median energy of events that would be detected resulting from using each of the EBL absorption models, approximately 100 GeV for both the “fast evolution” model of Stecker & de Jager (1998) and the Primack et al. (1999) model, and 150 GeV for the Primack et al. (2004) model. The derived upper limits of $E^2 dN/dE$, using these three absorption models are $1.6 \times 10^{-5} \text{ erg cm}^{-2}$ (for the first two models) and $6.7 \times 10^{-6} \text{ erg cm}^{-2}$ (for third one). These are shown as two separate arrows in Figure 4.

6. Discussion

The conclusive detection of TeV emission from GRBs would improve our current understanding not only of GRBs themselves, but also of a whole range of physical phenomena. Besides possibly allowing us to learn something about the magnetic fields and electron energies in the GRB environments, as in the case of blazars, it could also serve to distinguish particle acceleration models, constrain the models of the infrared photon density of the universe, and possibly to probe some more exotic phenomena such as quantum gravity (Amelino-Camelia et al. 1998). The number of GRBs visible to Milagro so far has been relatively small. The fraction of GRBs expected to be detected by Milagro depends

on many assumptions. As mentioned in the introduction, there are good theoretical as well as experimental reasons to expect GRBs to emit photons at GeV to TeV energies. Even if these photons were created at (and escaped) the source, however, one of the greatest limitations in their detection involves the attenuation due to the intergalactic background radiation. High energy γ -rays interact with intergalactic star light, creating electron positron pairs (Primack et al. 1999; Stecker & de Jager 1998; De Jager & Stecker 2002; Primack et al. 2004). The attenuation is a function of gamma-ray energy, the density and spectrum of the background radiation fields and, crucially, the distance to the source. Even at the relatively modest redshift of 0.5, the optical depth is greater than 1 at a few hundred GeV. Figure 3 shows the effect of the EBL on an $E^{-2.4}$ spectrum (shown, unabsorbed, as a straight line) at a redshift of 0.45, according to different models. Unfortunately, only three of the 25 GRBs studied here have a measured redshift, and of these, only GRB 010921, with a redshift of 0.45, was close enough for a significant fraction of photons to escape absorption.

Figure 5 compares the Milagro upper limits for a number of bursts with the observations made by BATSE and HETE (we show those for which a fluence in the lower energy bands was available). The quantity plotted is $E^2 dN/dE$. We have assumed an E^{-2} spectrum at the lower energies and an $E^{-2.4}$ spectrum for the Milagro energy range, evaluating it at 2.5 TeV. The circles represent HETE bursts while squares represent BATSE bursts. It is important to note that the absorption from the EBL has not been taken into account. Because the redshifts of these bursts are unknown, the Milagro upper limits cannot place tight constraints on the burst emission. For many bursts, the Milagro fluence limits are below those of HETE or BATSE, so that if the burst were known to be close, the limit would be constraining. GRB 010921 was the first HETE burst with a measured afterglow. The VHE limit from Milagro is the first which constrains the TeV flux rather than the distance to the source.

With the launch of Swift, we expect ~ 50 well-localized bursts in the Milagro field of view during the first two years, most of them with measured redshifts. There are currently 39 GRBs with known redshift (Greiner 2004). Figure 6 shows a histogram of these redshifts (left scale), with the cumulative distribution also shown on the plot (right scale). Approximately 20% of the measured redshifts are 0.5 or less. A sample of known low redshift GRBs, combined with the upgrades made to Milagro, increasing the effective area of Milagro and lowering its energy threshold, should allow us in the near future to improve greatly on the current results and shed some light on the nature of VHE emission from GRBs.

7. Conclusions

A search for very high energy emission from GRBs was performed with the Milagro observatory in the range of 50 GeV to 100 TeV. A total of 25 satellite-triggered GRBs were within the field of view of Milagro in the two year period between January 2000 and December 2001, including GRB 010921, at a known redshift of 0.45. No significant emission was detected from any of these bursts. 99% confidence upper limits on the fluence are presented.

Many people helped bring Milagro to fruition. In particular, we acknowledge the efforts of Scott DeLay, Neil Thompson and Michael Schneider. We have used GCN Notices to select raw data for archiving and use in this search, and we are grateful for the hard work of the GCN team, especially Scott Barthelmy. We thank Tim Donaghy and the rest of the HETE team for helpful comments as well as access to HETE data for GRB010921. This work has been supported by the National Science Foundation (under grants PHY-0075326, -0096256, -0097315, -0206656, -0245143, -0245234, -0302000, and ATM-0002744) the US

Department of Energy (Office of High-Energy Physics and Office of Nuclear Physics), Los Alamos National Laboratory, the University of California, and the Institute of Geophysics and Planetary Physics.

REFERENCES

- Amenomori, M. et al. 1996, *A&A*, 311, 919
- Amelino-Camelia, G. et al. 1998, *Nature*, 393, 763
- Atkins, R. et al. 2000a, *ApJ*, 533, L119
- Atkins, R. et al. 2000b, *Nucl. Instrum. Meth. A*, 449, 478
- Atkins, R. et al. 2003a, *ApJ*, 583, 824
- Atkins, R. et al. 2003b, *ApJ*, 595, 803
- Atkins, R. et al. 2004, *ApJ*, 608, 680
- Atteia, J. 2003, *astro-ph/0312371*
- Band, D., et al. 1993, *ApJ*, 413, 281
- Barraud, C. et al. 2003, *A&A*, 400, 1021
- Castro, S. M., et al. 2000, *GCN* 605
- Castro, S., Galama, T. J., Harrison, F. A., Holtzman, J. A., Bloom, J. S., Djorgovski, S. G.,
& Kulkarni, S. R. 2003, *ApJ*, 586, 128
- Connaughton, V., et al. 1997, *ApJ*, 479, 859
- Costa, E., et al. 1997, *Nature*, 387, 783
- Dall, T., et al. 2000, *GCN Circ.* 804
- de Jager, O. C. & Stecker, F. W. 2002, *ApJ*, 566,738
- De Pasquale, M., et al. 2003, *ApJ*, 592, 1018

- Dermer, C. D., Chiang, J., & Mitman, K. E. 2000, *ApJ*, 537, 785
- Dingus, B. L., 1995, *Astrophys. & Space Sci.*, 231, 187
- Dingus, B. L., 2001, in *High Energy Gamma Ray Astronomy*, ed. F. A. Aharonian and H. J. Volk, 2001, *AIP*, 558, 383
- Dingus, B. L., 2003, in *Gamma-Ray Bursts: 30 Years of Discovery*, ed. E. E. Fenimore and M. Galassi, 2003, *AIP*, 727, 131
- Djorgovski, S. G., et al. 2001, *GCN* 1108
- Fynbo, J. U. et al. 2001, *A&A*, 369, 373
- Galama, T. J., et al. 1998, *Nature*, 395, 670
- Gonzalez, M. M. et al. 2003, *Nature*, 424, 749
- Gorosabel, J., et al. 2000, *GCN Circ.* 803
- Greiner, J. 2004, <http://www.mpe.mpg.de/~jcg/grbgen.html>
- Helene, O. 1983, *Nucl. Instrum. Methods Phys. Res.*, 212, 319
- Hurley, K., et al. 2000, *GCN Circ.* 736
- Hurley, K., et al. 1994, *Nature*, 372, 652
- Kulkarni, S. R., et al. 1998, *Nature*, 395, 663
- Li, T. P., & Ma, Y. Q. 1983, *ApJ*, 272, 317
- Maiorano, E. et al. 2003, *astro-ph/0302022*
- Nikishov, A. I. 1961, *Zh. Eksp. i Teor. Fiz.*, 41, 549 (English translation: *Sov. Phys. JETP* 14, 392 [1962])

- Padilla, L., et al. 1998, *A&A*, 337, 43
- Pilla, R. P. & Loeb, A. 1998, *ApJ*, 494, L167
- Piro, L. 2000, *GCN Circ.* 703
- Preece, R. D., et al. 1998, *ApJ*, 506, L23
- Price, P. A., et al. 2001, *GCN Circ.* 1107
- Price, P. A., et al. 2003, *ApJ*, 584, 931
- Primack, J. R., Bullock, J. S., Somerville, R. S. & Macminn, D. 1999, *Astroparticle Physics*, 11, 93
- Primack, J. R., Bullock, J. S., & Somerville, R. S. 2004 in *Gamma 2004 Heidelberg*, ed. Aharonian, F. A. 2004
- Ricker, G. , et al. 2002, *ApJ*, 571, L127
- Smith, I. A., Tilanus, R. P. J., Wijers, R. A. M. J., Tanvir, N., Vreeswijk, P., Rol, E. & Kouveliotou, C. 2001, *A&A*, 380,81
- Sakamoto, T., et al. 2004, *ArXiv Astrophysics e-prints*, astro-ph/0409128
- Stecker, F. & de Jager, O. C. 1998, *A&A*, 334, L85
- van Paradijs, J., Kouveliotou, C. & Wijers, R. A. M. J. 2000, *ARA&A*, 38, 379
- Weekes, T. C. 2003, *Very High Energy Gamma-Ray Astronomy* (Bristol and Philadelphia: Institute of Physics)
- Zhang, B. & Mészáros, P. 2001, *ApJ*, 559, 110

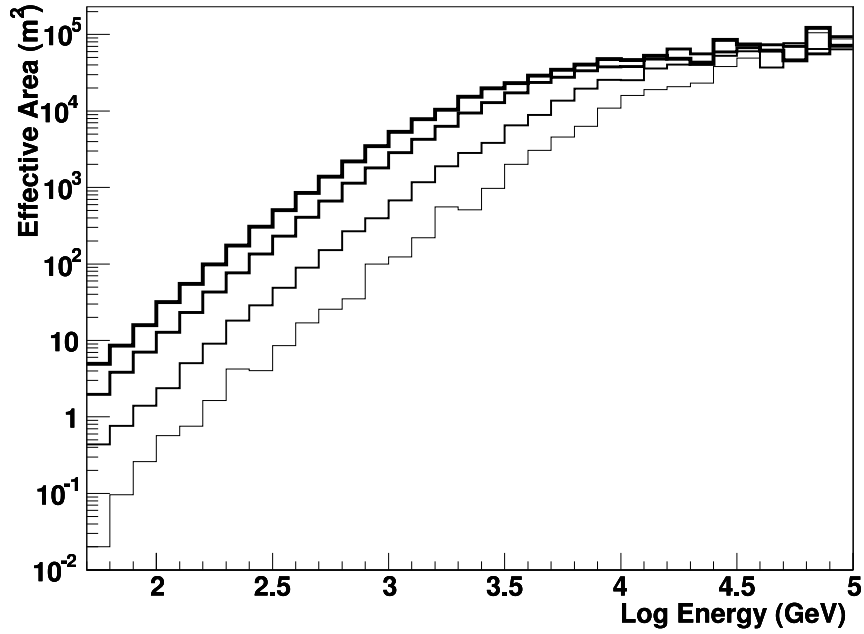


Fig. 1.— Effective area of Milagro to gamma rays as a function of energy for various zenith angles. The different lines reflect the effective area for different ranges of zenith angles (in decreasing order of thickness, 0° – 15° , 15° – 30° , 30° – 40° , and 40° – 45°) illustrating the drop suffered in effective area at energies below 1 TeV for large zenith angles.

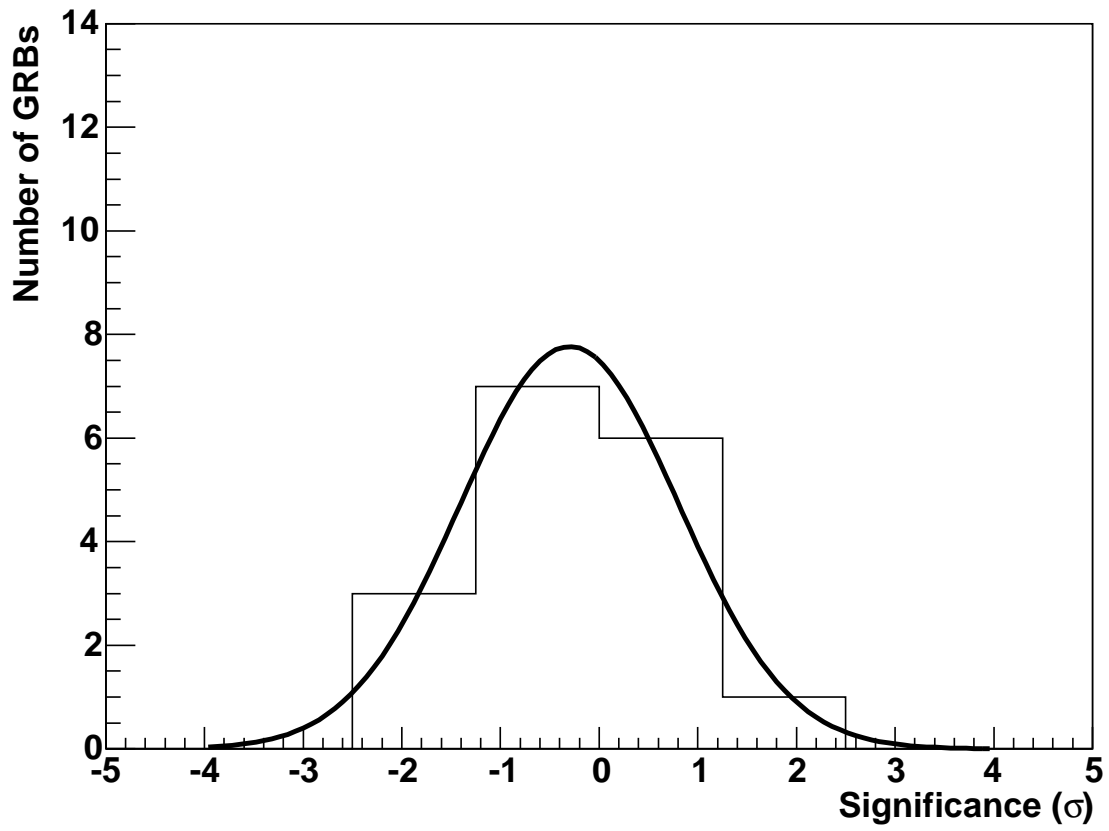


Fig. 2.— Distribution of significances of the 17 well-localized GRBs.

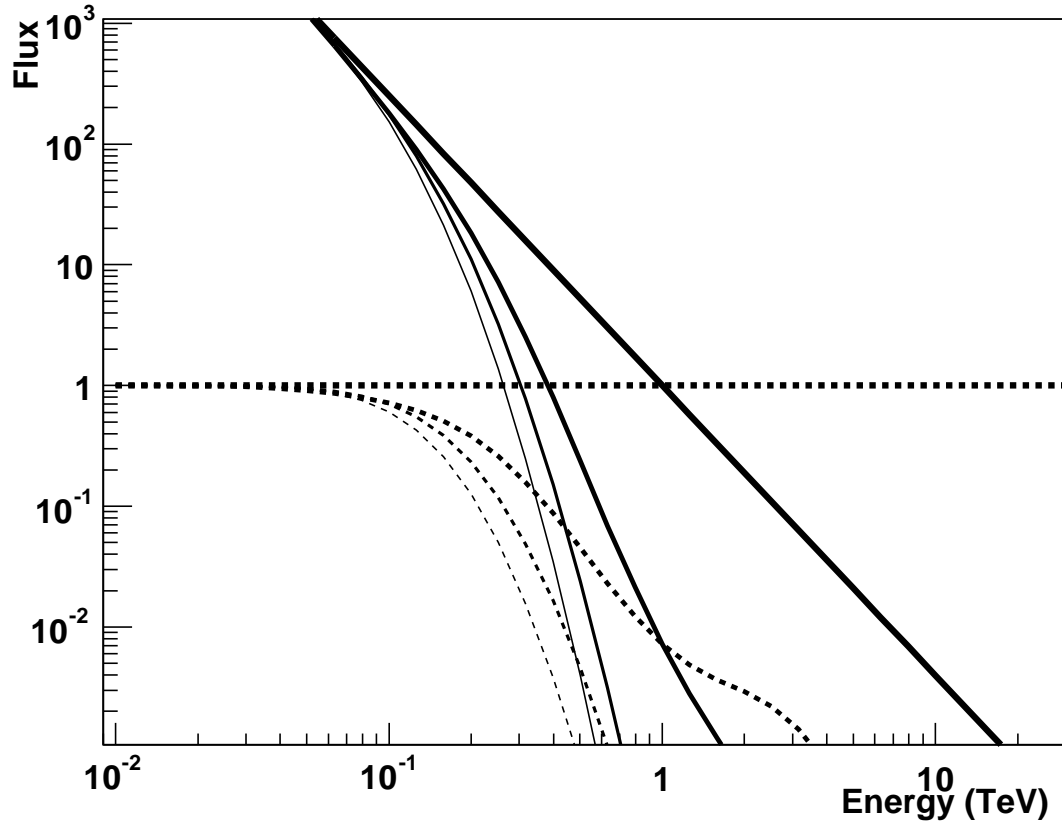


Fig. 3.— Effect of the EBL on an $E^{-2.4}$ spectrum for $z=0.45$. The solid lines represent (in order of decreasing thickness) the unabsorbed spectrum, the model of Primack et al. (2004), and the Baseline and Fast Evolution models of Stecker & de Jager (1998). The dashed lines represent the previous four curves divided by the unabsorbed spectrum; i.e. the attenuation factor.

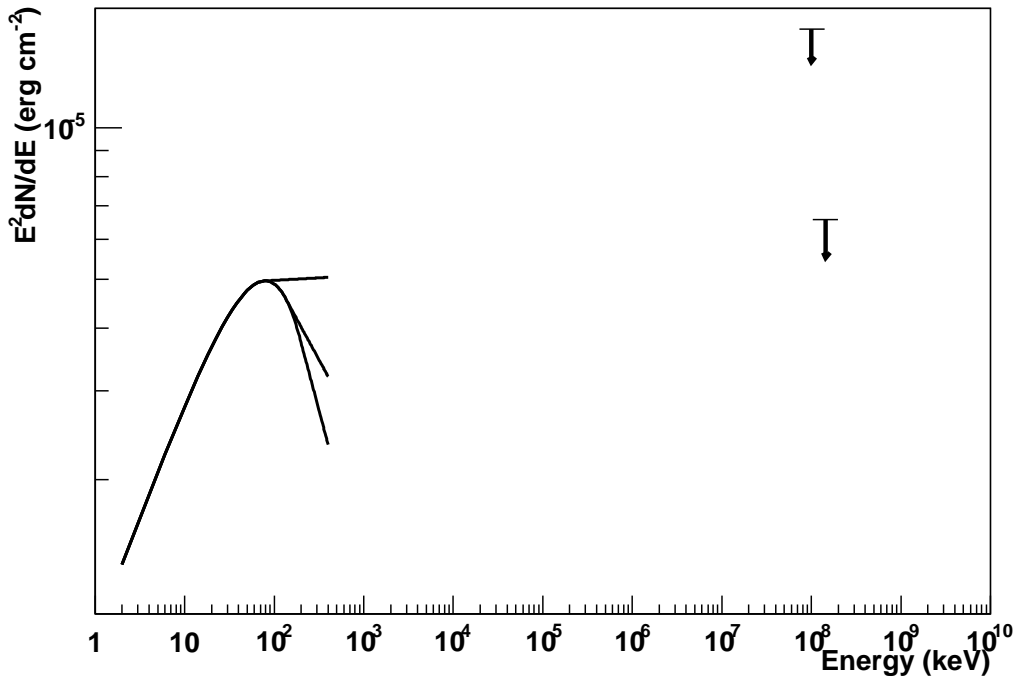


Fig. 4.— The GRB 010921 spectrum as measured by HETE (shown in the range 2–400 keV). The function is the result of fitting the data to the Band function. The high-energy power-law index β is unconstrained. We plot it for three values: -2.33, -1.99, and -2.67. The arrows are the upper limits from Milagro for various EBL absorption models, the lower energy one corresponding to the Stecker & de Jager (1998) and Primack et al. (1999) models (the results are very similar) and the slightly higher energy one corresponding to the more recent Primack et al. (2004) model. The energies at which these are evaluated are the respective median energies of the detected events and the quantity plotted is $E^2 dN/dE$.

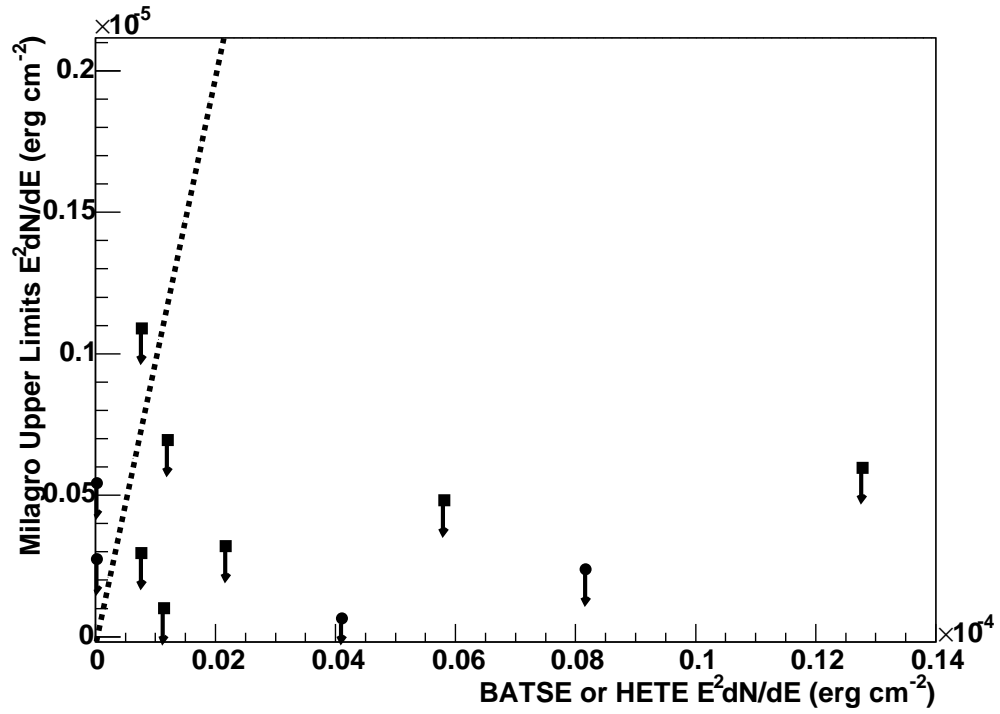


Fig. 5.— Comparison of BATSE (squares) and HETE (circles) fluences to Milagro upper limits. The bursts represented in this plot are: GRB 000113, 000212, 000226, 000302, 000317, 000331, 000508, 010613, 010921, 011130, and 011212. The dotted line represents the line $y=x$.

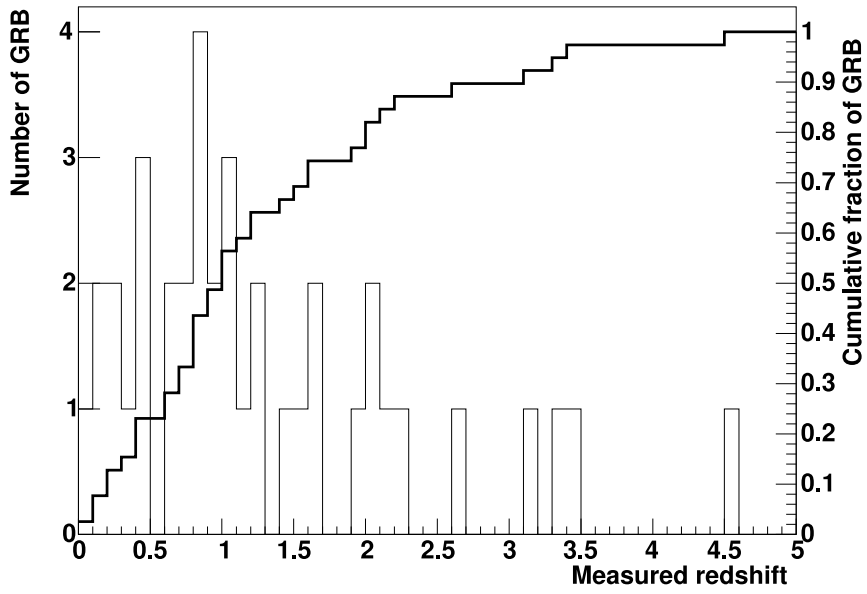


Fig. 6.— Distribution of the 39 currently measured redshifts, including bursts GRB 970228 through GRB 041006. The scale on the right refers to the cumulative distribution also shown in this plot.

Table 1. List of GRBs in the field of view of Milagro in 2000 and 2001

GRB	ID ²	Time ³	Pos. ⁴	Err. circ. ⁵	T90/Dur.(s)	z ⁷	ORX ⁸	θ ⁹	N_{ON} ¹⁰	N_{OFF} ¹¹	σ ¹²	N_{UL} ¹³	UL (T90/Dur.) ¹⁴	UL (5 min) ¹⁵
000113	7948	11556:34202.4	163.27,+19.89	5.0	370	20.9	471	423.2	...	95.8	5.5e-6	4.8e-6
000212	7987	11586:81065.2	16.09,+35.62	4.2	8	2.21	32	17.7	...	30.1	1.1e-6	5.0e-6
000226	7998	11600:13909.4	143.68,+29.82	4.5	10	31.5	25	11.4	...	27.9	3.4e-6	1.1e-5
000301C	8005R/I	11604:35497	245.09,+29.42	-	14	2.03	√/√.	37.6	11	10.3	0.2	12.0	2.6e-6	6.6e-6
000302	8008	11605:10225.1	58.20,+54.28	4.15	120	31.9	143	113.1	...	54.7	6.8e-6	1.2e-5
000317	8039	11620:77953.8	27.22,+32.66	5.5	550	6.39	1740	1625.9	...	208.0	7.9e-6	5.4e-6
000330	8057	11633:75449.4	358.31,+39.26	5.4	0.2*	30.0	3	0.3	...	9.8	1.0e-6	1.2e-5
000331	8061	11634:85421.8	32.00,+59.77	5.9	55	38.3	94	66.2	...	53.0	1.2e-5	2.1e-5
000408	I/8069	11642:9348.2	137.32,+66.58	0.5	2.5	...	×..	31.1	4	3.4	0.3	8.6	1.0e-6	6.7e-6
000508	8099	11672:77419.3	89.87,+2.41	4.3	30	34.1	25	15.3	...	24.0	3.7e-6	9.4e-6
000615	S	11710:22704	233.14,73.79	-	10	...	× × ×	39.0	3	7.2	-1.8	6.3	1.6e-6	8.0e-6
000630	I	11725:1853	221.81,+41.22	-	20	...	√×.	33.2	23	22.6	0.1	15.5	2.2e-6	6.7e-6
000727	I	11752:70956	176.00,+17.41	-	10	...	××.	40.8	5	6.2	-0.5	8.2	2.6e-6	1.2e-5
000730	I	11755:255	191.29,+19.27	-	7	19.2	8	13.9	-1.7	7.9	4.2e-7	2.7e-6
000926	I	11813:85773	256.06,+51.78	-	25	2.04	√√√	15.9	60	56.8	0.4	25.2	1.2e-6	3.4e-6
001017	I	11834:80346	272.18,-2.99	0.5	10	42.1	2	4.6	-1.3	6.1	2.2e-6	1.0e-5
001018	I	11835:61114	198.54,+11.81	0.5	31	...	√.	31.8	31	31.5	-0.1	16.9	2.1e-6	6.8e-6
001019	I	11836:86375	257.93,+35.34	-	10	...	×..	19.5	27	21.1	1.2	20.9	1.1e-6	1.1e-6
001105	I	11853:59128	195.3,+35.49	-	30	...	×..	8.5	87	76.2	1.2	35.6	1.4e-6	2.0e-6
010104	I	11913:62489	267.4,+18.23	0.5	2	19.8	3	3.3	-0.2	7.5	4.0e-7	2.8e-6
010220	S	11960:82267	39.4,+61.7	-	150	...	××.	27.0	155	168.8	-1.1	24.9	2.1e-6	3.0e-6
010613	I/H	12073:27234	255.18,+14.27	-	152	24.7	277	280.5	-0.2	40.7	2.9e-6	5.1e-6
010921	I/H	12173:18950.6	344.0,+40.93	-	24.6	0.45	√/√.	10.4	61	65.4	-0.6	20.2	8.0e-7	2.2e-6
011130	H	12243:22775.7	46.4,+3.8	-	83.2	...	× × ×	33.7	93	100.9	-0.8	23.0	3.4e-6	8.3e-6
011212	H	12255:14642	75.051,+32.13	-	84.4	33.0	132	113.1	1.7	43.8	6.7e-6	1.2e-5

Note. — 2) BATSE ID, when known, otherwise: R – *RXTE*, I – IPN, H – *HETE*, S – *BeppoSAX*; 3) Time of burst, TJD: seconds; 4) ra,dec in degrees; 5) Error circle in degrees (a dash implies error is small compared to the Milagro PSF); 7) redshift (when known); 8) afterglow observed: O – Optical/IR, R – Radio, X – X-ray; 9) Zenith angle, in degrees; 10) Milagro number of counts on source; 11) Estimated number of background counts; 12) Statistical significance of the excess (in standard deviations); 13) 99% Upper Limit on the number of counts coming from the source; 14) 99% Upper Limit on the fluence (0.25–25 TeV), in ergs cm⁻² for the duration in column 6; 15) 99% Upper Limit on the fluence (0.25–25 TeV), in ergs cm⁻² for a duration T = 5 min. *) Estimate.